Controls of erosional denudation in the orogen on foreland basin evolution: The Oligocene central Swiss Molasse Basin as an example

Fritz Schlunegger[1] and Teresa E. Jordan
Department of Earth Sciences, Cornell University, Ithaca, New York

Eva Maria Klaper
Geologisches Institut, Universität Bern, Bern, Switzerland

Abstract. A high-resolution three-dimensional reconstruction of the 25-m.y.-old central Swiss Molasse Basin reveals two sedimentary domains separated by a ~5-km-wide floodplain. The proximal domain of the basin attained a width of 20 km, and its basement is steeply flexed (6°-7° dip). Petrographic data indicate that it was filled by sediment from the Rigi dispersal system derived from the central Alps of eastern Switzerland and by locally sourced bajadas. In contrast, the distal sedimentary domain, located farther north, was gently dipping (<2°) and was filled by the meandering Lac Léman and Honegg dispersal systems. Chronological data reveal that sedimentation in the northern proximal part of the basin started at ~27 Ma, when sediment supply to the basin started to increase. Deflection of the foreland plate at ~25 Ma is successfully simulated by flexural modeling of the thrust load and the sediment load. The model reveals that the Lac Léman and Honegg dispersal systems are located on a buried flexural bulge. Furthermore, it shows that burial and suppression of the flexural bulge at ~27 Ma as well as an increase of the basin wavelength were controlled by the contemporaneous increase in the sediment supply rate of the Rigi system. The model presented suggests that the tectonic subsidence of the Molasse Basin was mainly controlled by tectonic events in the northern part of the orogen, within ~70 km distance from the tip of the orogenic wedge. Crustal thickening in this part of the orogen is reflected in the proximal Molasse by sedimentary cycles characterized by an increase in the sediment accumulation rates up section and by the presence of locally sourced bajada fans at the top of each cycle. Although south vergent back thrusting along the Insubric Line ~150 km south of the foreland basin contributed little to flexure, it resulted in an increase of the sediment supply to the foreland basin. This is reflected in the Molasse by coarsening and thickening upward trends, an increase of the basin wavelength, basinward shifts of the depocenters of the dispersal systems, and uplift and erosion of the proximal basin border.

[1]Now at Insitut für Geowissenschaften, Friedrich-Schiller-Universität Jena, Jena, Germany.

1. Introduction

Foreland basins have been extensively studied because they chronicle in great detail the tectonic and denudation history of the bounding mountain belt [*Jordan*, 1981]. Whereas it is now widely understood that crustal and/or subcrustal loading controls basin subsidence, relationships between erosional denudation and the geometrical and architectural evolution of foreland basins have been postulated but not yet adequately investigated [*Flemings and Jordan*, 1989, 1990; *Jordan and Flemings*, 1991; *Paola et al.*, 1992].

A successful reconstruction of the relationships between crustal thickening and erosional denudation of the orogen and the evolution of the adjacent foreland basin requires (1) knowledge of the structural geometries and the deformation history in the hinterland, (2) cooling ages to assess the long-term rate and the spacial history of denudation, (3) a high-resolution reconstruction of the architecture of the foreland basin, (4) petrographic data from the foreland basin to locate the source area, and (5) knowledge of the mechanical properties of the foreland plate [*DeCelles and Mitra*, 1995]. The Oligo-Miocene Alps/Molasse Basin, which is among the best understood orogen-basin systems in the world, meets most of these requirements [*Pfiffner*, 1986; *Schmid et al.*, 1996]. On the basis of flexural modeling and high-resolution magnetostratigraphy, *Sinclair et al.* [1991], *Royden* [1993], and *Schlunegger et al.* [1997a, b] revealed the stratigraphical and geometrical reponse of the Molasse Basin to crustal loading in the Alpine orogen. Using a forward diffusion model of mountain belt uplift and erosion, *Sinclair and Allen* [1992] proposed the concepts of linking erosional denudation in the hinterland to basin architecture.

In this paper, we reconstruct the three-dimensional architecture and the deflection of the 25-m.y.-old Molasse Basin of central Switzerland. The reconstruction is based on a compilation of published chronological and stratigraphical data and on new sedimentological and petrographical studies carried out for three outcrop sections. Further attention is focused on restoring the Alpine thrust load and the sediment load of the Molasse Basin at ~25 Ma. This guess of the load distribution in the late Oligocene as well as determination of the foreland plate deflection are used to estimate the mechanical properties of the foreland plate by flexural modeling. The result of these calculations allows us to evaluate to what extent the sediment load controlled the basin subsidence. This evaluation will be

used to discuss the significance of sediment supply as a control on the geometrical and stratigraphical evolution of the central Swiss Molasse Basin in the early Chattian (30-25 Ma) [*Schlunegger et al.*, 1996].

2. Geological Setting

The present-day Alps are the result of the continent-continent collision between the Adriatic promontory of Africa and the European plate that started in the Late Cretaceous [*Lihou and Allen*, 1996]. The Alps form a doubly vergent compressional orogen that consists of thin-skinned and thick-skinned mostly unmetamorphosed thrust sheets at their external flanks and high-grade metamorphic rocks in their core [*Laubscher*, 1990; *Schönborn*, 1992; *Pfiffner*, 1992; *Schmid et al.*, 1996] (Figure 1a). On the basis of the geological interpretation of geophysical data, *Laubscher* [1990], *Pfiffner* [1992] and *Schmid et al.* [1996] could show that collision between the two plates occurred by insertion of the Adriatic lower crust into the interface between the south dipping European lower crust and the European upper crust (Figure 1b).

In the north, the present-day Alpine edifice consists of the Helvetic zone, which is subdivided into a lower Infrahelvetic complex (Aar massif and its autochthonous - parautochthonous cover) and an upper Helvetic (sensu stricto) complex (Helvetic thrust nappes), separated by the north vergent basal Helvetic thrust (Figure 1b). In the eastern part of the Swiss Alps, the Helvetic zone is overlain by a piggyback stack of Penninic and Austroalpine sedimentary nappes (Figure 1a). The Central Alps comprise a stack of north vergent Penninic and Austroalpine sedimentary and crystalline nappes. They are separated from the south verging Southern Alps [*Schönborn*, 1992] by the mainly E-W striking Insubric Line (Figure 1a). This suture partly accommodated the identation of the Adriatic promontory by steep south directed synmagmatic reverse faulting and right-lateral strike-slip movements [*Pfiffner*, 1992; *Schmid et al.*, 1996] (Figure 1b).

The early Chattian (30-25 Ma) and partly the Rupelian (<30 Ma) deposits of central Switzerland, which are the focus of this paper, are part of the Oligo/Miocene north Alpine foreland basin, which evolved as a response to the tectonic load of the evolving Alpine thrust wedge (Figure 2) [*Homewood et al.*, 1986; *Sinclair et al.*, 1991; *Schlunegger et al.*, 1997a]. The sedimentological development of the north Alpine foreland basin can be described in terms of an early deepwater stage and a later shallowwater/continental stage which have been referred to as "Flysch" and "Molasse" in the classic Alpine literature (see discussions of *Sinclair et al.* [1991] and *Sinclair and Allen* [1992]). The "Molasse" has been traditionally divided into four lithostratigraphic units, for which the conventional German abbreviations are used in this paper (Figure 2) [*Matter et al.*, 1980; *Keller*, 1989]: Lower Marine Molasse (UMM), Lower Freshwater Molasse (USM), Upper Marine Molasse (OMM), and Upper Freshwater Molasse (OSM). They form two shallowing upward megasequences. The first megasequence comprises the Rupelian UMM, which is followed by the Chattian and Aquitanian fluvial clastics of the USM. The second megasequence, starting with the Burdigalian transgression, consists of shallow marine sandstones (OMM), which interfinger with major fan deltas adjacent to the thrust front

[*Berli*, 1985; *Keller*, 1989; *Hurni*, 1991; *Schlunegger et al.*, 1993]. It ends with Serravalian fluvial clastics of the OSM.

The Rupelian to early Chattian deposits of central Switzerland compose the Lower Marine Molasse group (UMM) and the lower Lower Freshwater Molasse group (USM I of *Schlanke* [1974]). The UMM forms the transition from the early underfilled "Flysch" stage of the north Alpine foreland basin to the overfilled "Molasse" stage [*Sinclair et al.*, 1991; *Sinclair and Allen*, 1992]. It consists of deep marine turbidites at its base, overlain by a regressive sequence comprising offshore mudstones, nearshore sandstone/mudstone alternations, and shoreface sandstones [*Diem*, 1986]. At the Alpine thrust front, contemporaneous fan deltas interfingered with the peri-alpine sea (O. Kempf, personal communication, 1995). The USM I consists of bajadas and alluvial megafans at the tip of the orogenic wedge, which pass down current into conglomerate channel belt, sandstone channel belt and floodplain deposits [*Schlunegger et al.*, 1997b].

At the Alpine border, the Oligocene Molasse is present in a stack of southward dipping thrust sheets (Subalpine Molasse), which in turn are overlain by the Helvetic thrust nappes (Figure 2). The Plateau Molasse, which represents the more distal part of the basin, is mainly flat lying and gently dips toward the Alpine orogen. However, synsedimentary underplating of USM thrust sheets beneath the Plateau Molasse resulted in back thrusting of the latter unit and in the development of a classical triangle zone just north of the Subalpine zone [*Vollmayr and Wendt*, 1987; *Stäuble and Pfiffner*, 1991].

Schlunegger et al. [1997b] reconstructed the two-dimensional architecture of the central Swiss Molasse at ~25 Ma, using the thicknesses and the sedimentological data from an outcrop section (Rigi) and three boreholes (Entlebuch-1, Boswil-1, and Hünenberg-1; Figure 2). These authors demonstrated that at ~25 Ma the Molasse Basin consisted of two parts (northern and southern sedimentary domains) that are separated by a ~5-km-wide floodplain (Figure 3). The southern more proximal part of the basin attained a restored width of ~20 km and dipped as much as $6°-7°$ south at the Alpine thrust front. There the sedimentary fill consists of a ~3700-m-thick shallowing, coarsening, and thickening upward megasequence, comprising the marine deposits of the UMM at its base (~100 m), overlain by the floodplain, conglomerate channel belt, alluvial megafan, and bajada depositional systems (~3600 m) (Figure 3a). In contrast, the northern more distal sedimentary realm was ~30 km wide, and its basement dipped gently southward (< $2°$ south). There the basin fill is represented by a <500-m-thick series comprising the sandstone meander belt and floodplain depositional systems, and no coarsening upward trend is present. At the Oligocene/Miocene boundary, uplift and erosion occurred in the southern proximal part of the basin, and the depocenters of the depositional systems shifted 12 km farther north into the more distal reaches [*Schlunegger et al.*, 1997b]. Note that south of the area of Entlebuch-1, the change of dip of the basement increased (Figures 3a and 3b).

Determination of the conglomerate clast population and the heavy mineral suite of sandstones reveals the presence of five dispersal systems (Figures 3b and 3c) [*Füchtbauer*, 1959, 1964; *Gasser*, 1968; *Müller*, 1971; *Stürm*, 1973; *Schlunegger et al.*, 1997b]. The depocenter of the first system, referred to as Lac Léman river, was located at the western end of the Molasse
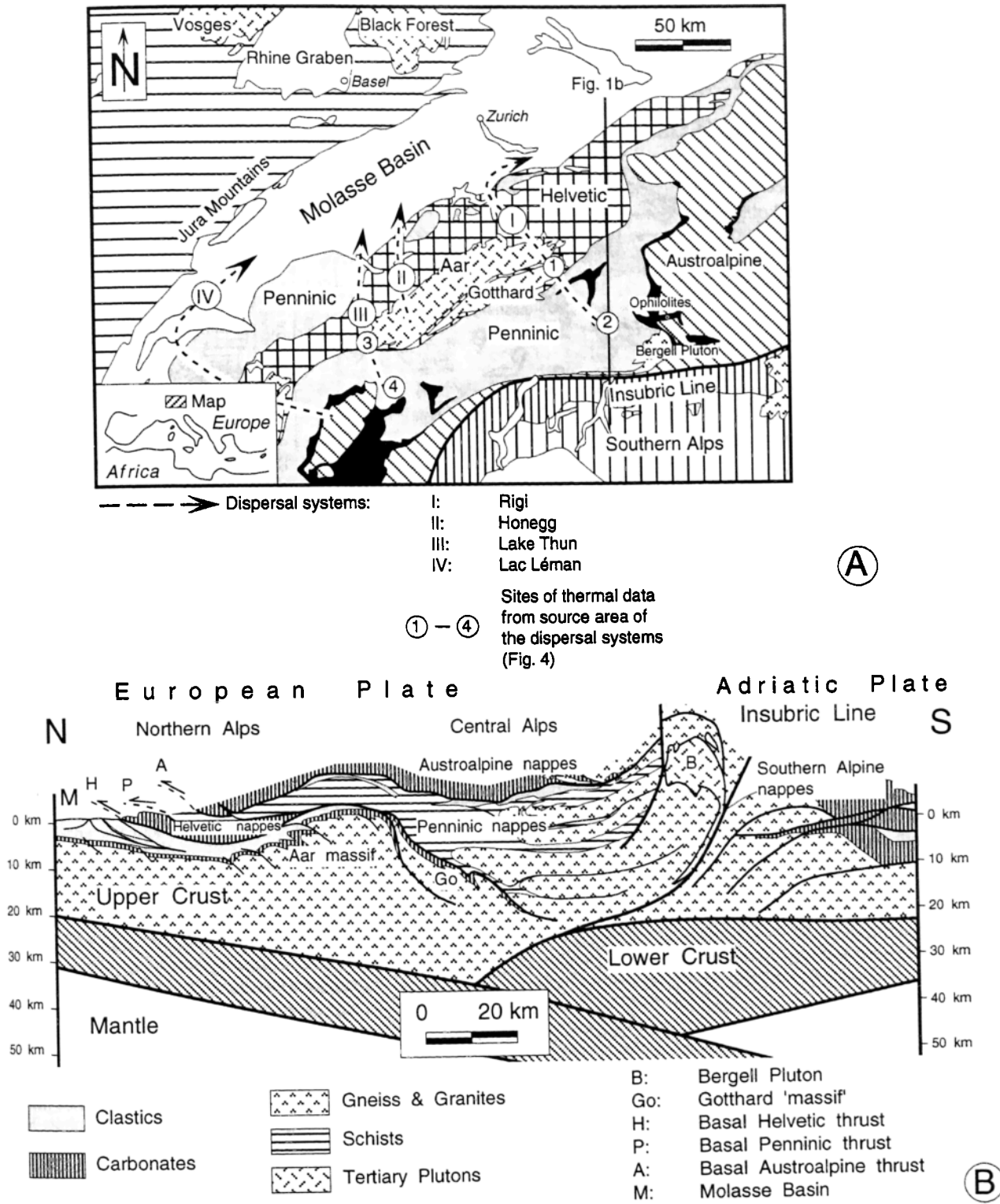
Figure 1. (a) Geological map of the Oligo-Miocene Swiss Molasse Basin and the adjacent Alpine orogen. The major tectonic units are labeled. The map also shows the location of the major north Alpine dispersal systems that fed the Molasse Basin of the study area. The numbers 1-4 represent locations of the thermal data shown in Figure 4. Note that in the eastern Alps, the Penninic and Austroalpine nappes are part of the northern Alps. In the analyzed cross section, however, they crop out in the central Alps south of the Aar massif. (b) Synthetic cross section through the present-day Alpine hinterland. The eroded Penninic and Austroalpine nappes are projected into the cross section to illustrate the architecture of the Alpine edifice prior to erosion (modified after *Schmid et al.* [1996]).
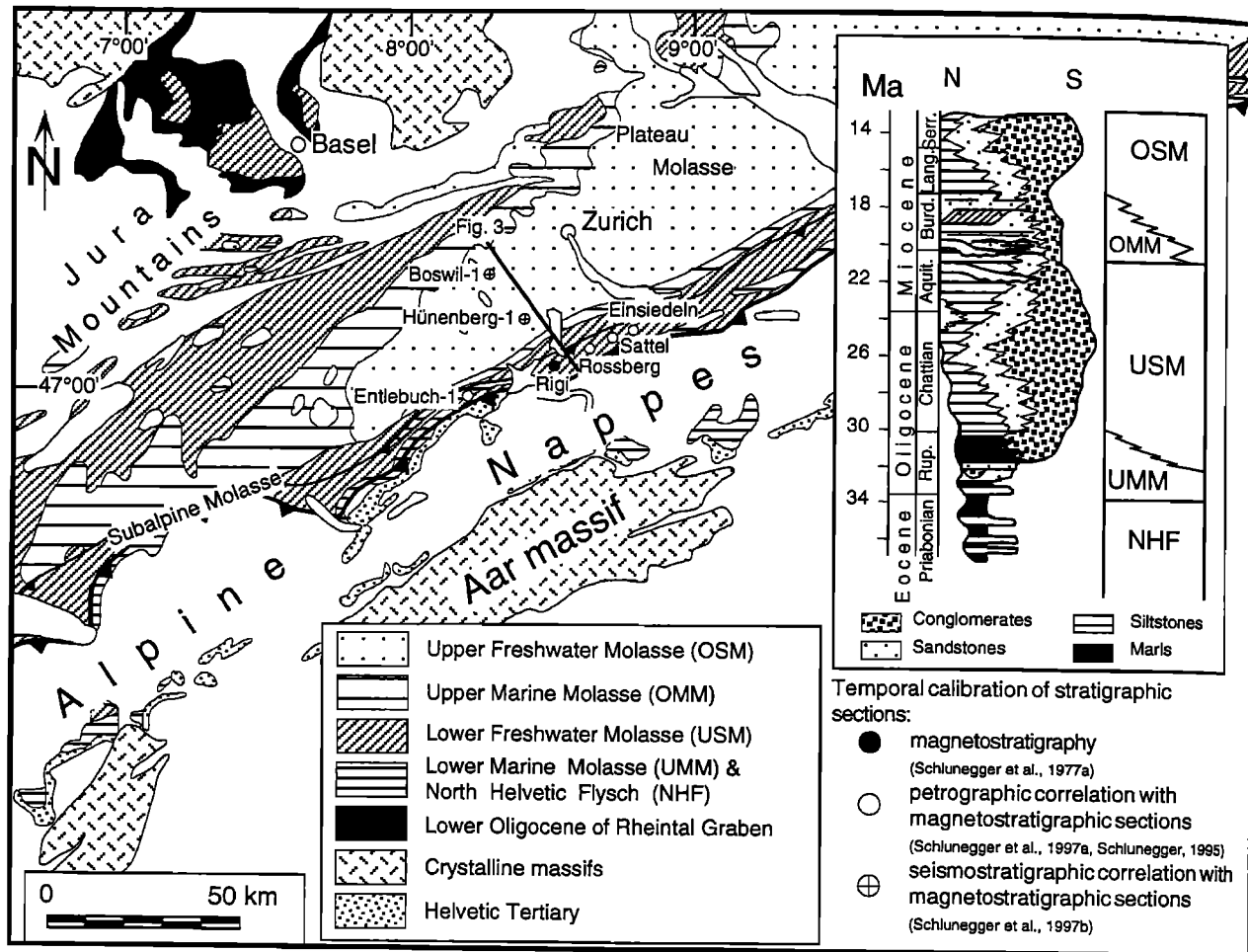
Figure 2. Geological map of the Oligo-Miocene Swiss Molasse Basin and the adjacent Alpine orogen with a general stratigraphy of the foreland basin and the location of the studied transect, the boreholes, and the analyzed sections.

Basin ~150 km southwest of the study area, from where it flowed eastward along the featheredge of the basin to the analyzed cross section (Figure 3c). The Lac Léman system was fed by the second system, the transverse Lake Thun dispersal system that originated in the Central Alps of western Switzerland and that entered the basin 80 km southwest of the study area (Figures 1a and 3c). The third dispersal system, referred to as Honegg river, was derived from the Central Alps ca. 55 km farther east and interfingered with the Lac Léman system in the Zurich area (Figures 1a and 3c). These dispersal systems occupied the northern sedimentary domain of the Molasse in the analyzed cross section (Figure 3b). The strata in the southern depositional domain were deposited by the Rigi dispersal system and by local systems (Figures 3b and 3c). The Rigi river was derived from the Central Alps of eastern Switzerland and deposited the conglomerates and mudstones in the proximal part of the analyzed transect (Figure 1a). The local dispersal systems, however, were sourced from the frontal Alpine units and formed the bajadas bordering the Alpine thrust front (Figures 3b and 3c).

In order to extend the initial two-dimensional reconstruction of the 25-m.y.-old basin architecture into the third di-

mension, three additional representative sections (Rossberg, Sattel, and Einsiedeln) were analyzed for sedimentary facies, paleoflow directions, and petrofacies. These sections are located in the Subalpine Molasse adjacent to the Alpine thrust front (Figure 2) and comprise the deposits of the southern depositional domain. Each of these sections measures between 2600 and 3600 m in thickness and comprises a ~600 -to 1200-m-thick succession of predominantly mudstones at the base, overlain by alternating conglomerates and mudstones [Müller, 1971; Stürm, 1973; Schlanke, 1974].

3. Three-Dimensional Reconstruction of the Foreland Basin Architecture and Tectonic Controls

3.1. Methods

Floodplain, conglomerate channel belt, and bajada depositional systems were differentiated following Schlunegger et al. [1997b]. The thickness of each unit was calculated based on measured dip angles of the beds, new mapping, and a compila-
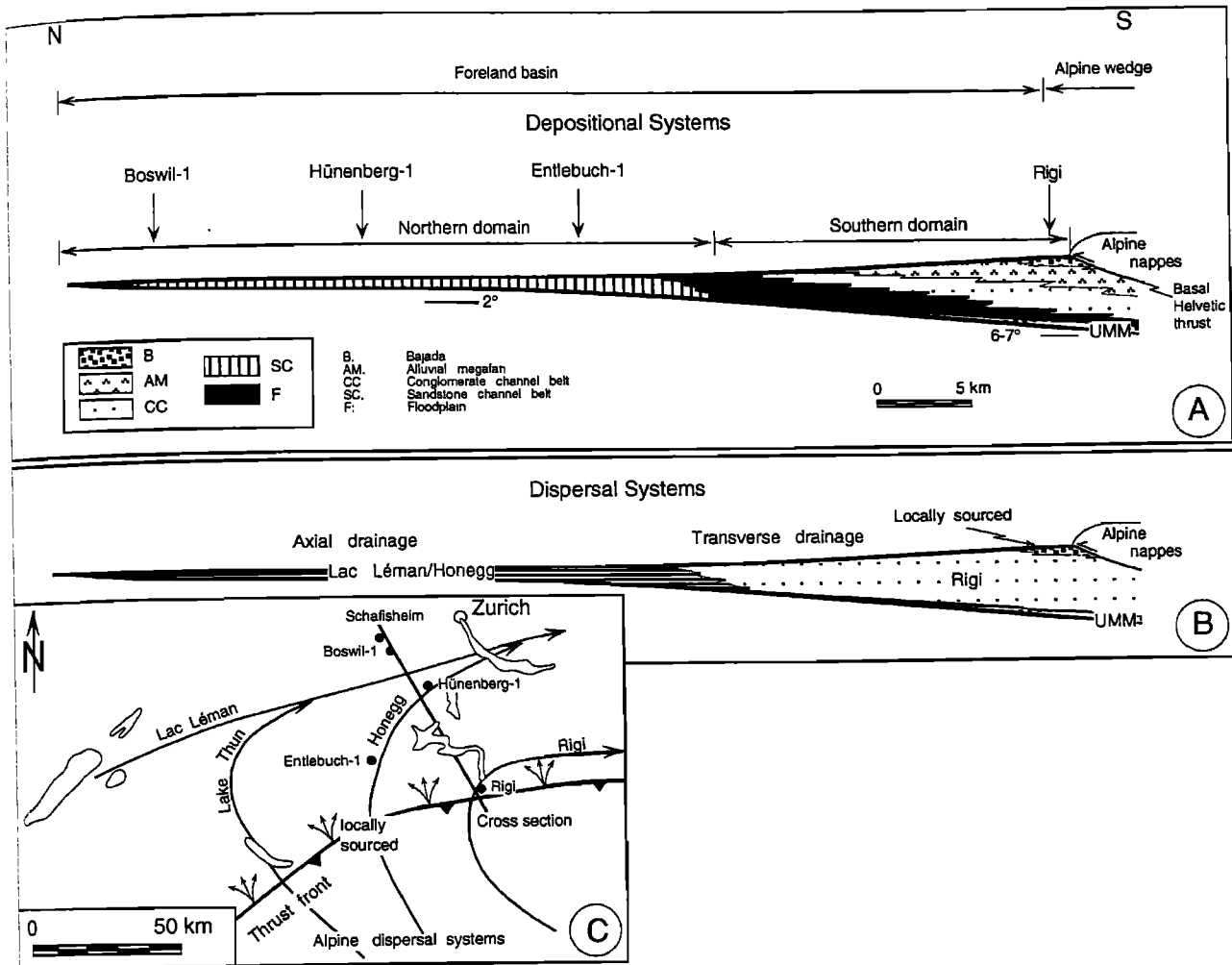
Figure 3. Paleogeographic diagram for the time interval between 30 and 25 Ma, showing (a) the basin geometry and architecture, (b) the location of the dispersal systems, and (c) the drainage pattern [*Schlunegger et al.*, 1997b].

tion of the geological maps of *Buxtorf et al.* [1916], *Ottiger et al.* [1990], *Müller* [1971], *Stürm* [1973], *Schlanke* [1974], and *Schlunegger et al.* [1997a].

Paleocurrents were determined from furrows, large-scale (>0.5 m) trough cross beds, and imbricate clasts in the conglomerates. The tectonic tilt in the Subalpine Molasse was removed in order to determine the paleoflow direction at the time of deposition. Petrofacies were determined by giving special attention to the first appearance of distinctive clasts.
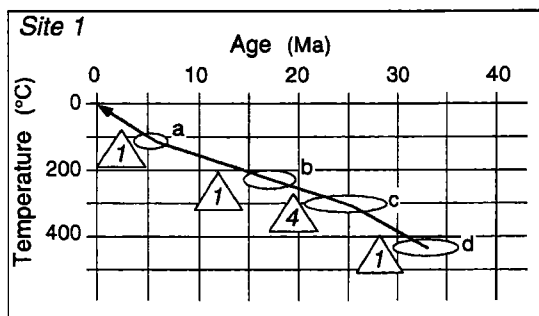
We sought to estimate the relative abundance of sediment supply to the basin through time through use of thermochronological data for four sites located in the source area of the Alpine rivers [*Hunziker et al.*, 1992] (Figures 1a and 4). If the pre-20-Ma exhumation in this part of the orogen was mainly controlled by erosional denudation which we will assume to be true [e.g. *Steck and Hunziker*, 1994], the thermal data are an indirect measurement of the sediment supply to the basin. Indeed, a careful estimate of the sediment supply to the basin would require a compilation of cooling ages that covers the whole source area. However, our simplistic approach based

on four sites is justified because (1) except for a few cases we used multiple temporal calibrations for each thermal stage (Figure 4), (2) we added error bars that comprise uncertainties in the temporal calibration of each thermal stage and uncertainties in the closure temperatures of the different radiometric systems, and (3) we used the thermal data only to qualitatively estimate the change of sediment supply to the basin.
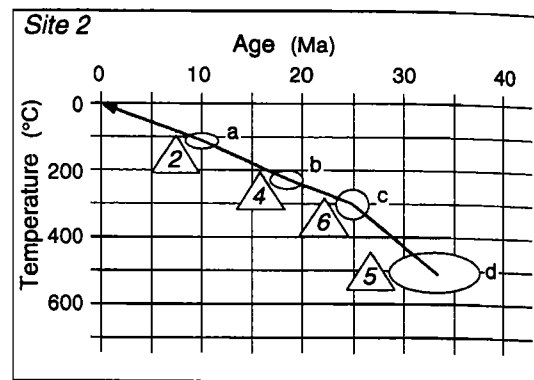
3.2 Results

Mapping of lithofacies and petrofacies reveals that the deposits of the Rigi and locally sourced dispersal systems, found in the southern sedimentary domain (Figure 3b), are present in all the analyzed sections adjacent to the Alpine border between Einsiedeln and Rigi (Figure 5a). At Rigi, a well-developed coarsening and thickening upward megasequence, comprising the floodplain, conglomerate channel belt, and alluvial megafan/bajada depositional systems, together with the change from initially axial to transverse paleoflow directions, indicate fan progradation (Figure 5a). Along strike from west
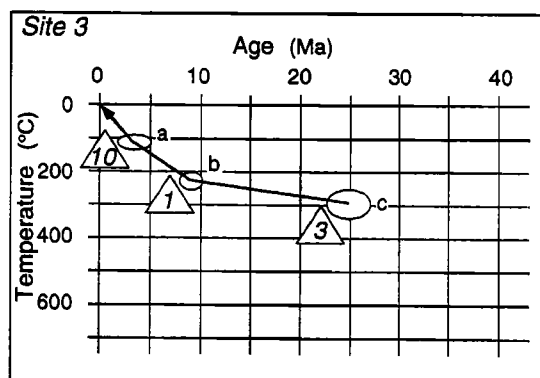
Source area of the Rigi system

Site 1

Age (Ma)

0   10   20   30   40

Temperature (°C)

0
200
400

a
b
c
d

Gotthard 'massif'

/4\ number of measurements

Site 2

Age (Ma)

0   10   20   30   40

Temperature (°C)

0
200
400
600

a
b
c
d

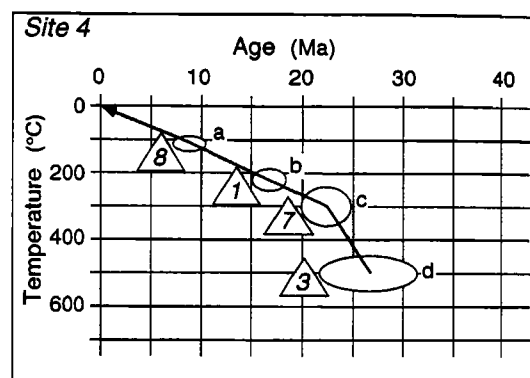Penninic nappes, East

/5\ number of measurements

Source area of the Honegg-Thunersee (sites 3 & 4)
and the Lac Léman systems (site 4)

Site 3

Age (Ma)

0   10   20   30   40

Temperature (°C)

0
200
400
600

a
b
c

Aar massif, West

/3\ number of measurements

Site 4

Age (Ma)

0   10   20   30   40

Temperature (°C)

0
200
400
600

a
b
c
d

Penninic nappes, West

/3\ number of measurements

Figure 4. Thermal evolution of the catchment area of the Rigi and Lake Thun systems. The cooling ages for gneiss samples form the Gotthard "massif" were determined with the following methods: (method a) apatite and (method b) zircon fission track [*Michalski and Soom*, 1990], (method c) Rb-Sr and K-Ar on biotite [*Soom*, 1990; *Dempster*, 1986], and (method d) formation ages of hornblende [*Steiger*, 1964; *Deutsch and Steiger*, 1985]. The thermal data of the Penninic nappes in the east represent (method a) apatite and (method b) zircon fission track ages, (method c) K-Ar and Rb-Sr ages measured on biotite, and (method d) formation ages of muskovite [*Jäger et al.*, 1967; *Giger*, 1991; *Hurford*, 1991; *Hunziker et al.*, 1992]. For the Aar massif, the fission track ages of (method a) apatite and (method b) zircon and the formation ages of (method c) biotite are taken from *Dempster* [1986] and *Michalski and Soom* [1990]. A full discussion of the thermal evolution of the Penninic nappes in the west was published by *Hurford* [1986], *Hurford et al.* [1989] and *Engi et al.* [1995] ((method a) apatite and (method b) zircon fission track data, (method c) Rb-Sr and K-Ar cooling ages measured on biotite, and (method d) formation ages of metamorphic fabrics).

to east, the basal floodplain depositional system thickens from initally 400 m at Rigi to approximately 1200 m at Einsiedeln (Figure 5a). Eastward thickening of the floodplain facies is offset by a thinning of the conglomerate facies (conglomerate channel belt, alluvial megafan, and bajada depositional systems) from 2800 m at Rigi to <1000 m at

Einsiedeln. Furthermore, maximum clasts of >50 cm are exposed at Rigi, from where they fine to <20 cm at Einsiedeln. This lateral change of facies indicates that the point of entry of Rigi river into the basin might have been located at Rigi, from where it flowed eastward toward Einsiedeln as supported by paleoflow directions (Figure 5a).
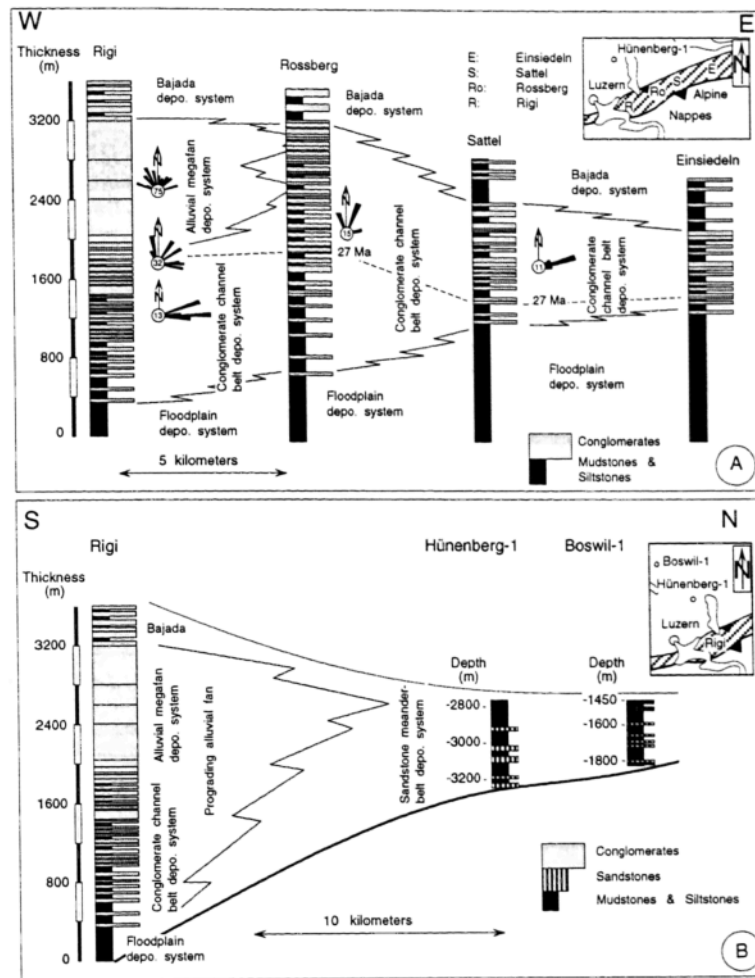
Figure 5. (a) Stratigraphy and sedimentology of the analyzed sections located in the southern sedimentary domain, revealing the along-strike sedimentological change of the Rigi dispersal system. Solid lines indicate facies boundaries. Dashed lines show chronologic correlation. (b) Stratigraphy and sedimentology of three representative sections located in the southern (Rigi) and northern (Hünenberg-1 and Boswil-1) sedimentary realms.

The deposits of the Lac Léman and Honegg dispersal systems, found in the northern depositional domain at Hünenberg-1 and Boswil-1, are an alternation of sandstones, siltstones, and mudstones that reflect the presence of a sandstone meander belt depositional system (Figure 5b) [*Schlunegger et al.*, 1997b]. In contrast to the more proximal southern part of the basin, however, no vertical sedimentary trend is detected in the Hünenberg-1 and Boswil-1 wells (Figure 5b).

Reconstruction of the facies relationships in the detailed temporal framework provided by magnetostratigraphy at Rigi reveals that sedimentation of fluvial deposits started at ~30 Ma at the proximal basin border (Rigi section, Figure 6a). Correlation of the Hünenberg-1 and Boswil-1 wells by magnetostratigraphy and seismostratigraphy to the Rigi section [*Schlunegger et al.*, 1997a, b] shows that at Hünenberg-1 and Boswil-1 accumulation of sediment began at ~27 Ma (Figure 6b). Also at ~27 Ma, the alluvial megafan depositional system started at Rigi, associated with the first appearance of crys-

talline clasts derived from the Central Alps of eastern Switzerland (Figure 6a). Farther east, between Rossberg and Einsiedeln (Figure 6a), the same petrographic change coincides with initiation of coarsening and thickening upward trends (Figure 5a), suggesting enhanced fan progradation at that time. Furthermore, the magnetic-polarity-based chronology established at Rigi indicates that at ~27 Ma, the sediment-accumulation rate increased from initially 700 m/m.y. between 30 and 27 Ma to more than 1000 m/m.y. between 27 and 25 Ma [*Schlunegger et al.*, 1997a].

The three-dimensional architecture of the Oligocene Molasse Basin reveals that the Molasse deposits onlap progressively the unconformity above the top of the Mesozoic carbonates (Figures 6b and 7), resulting in an angular unconformity between the foreland deposits and the underlying basement. However, between 30 and 28 Ma, sediments were predominantly deposited in the southern, more proximal part of the basin (Figures 6b and 7). There the angle of unconfor-
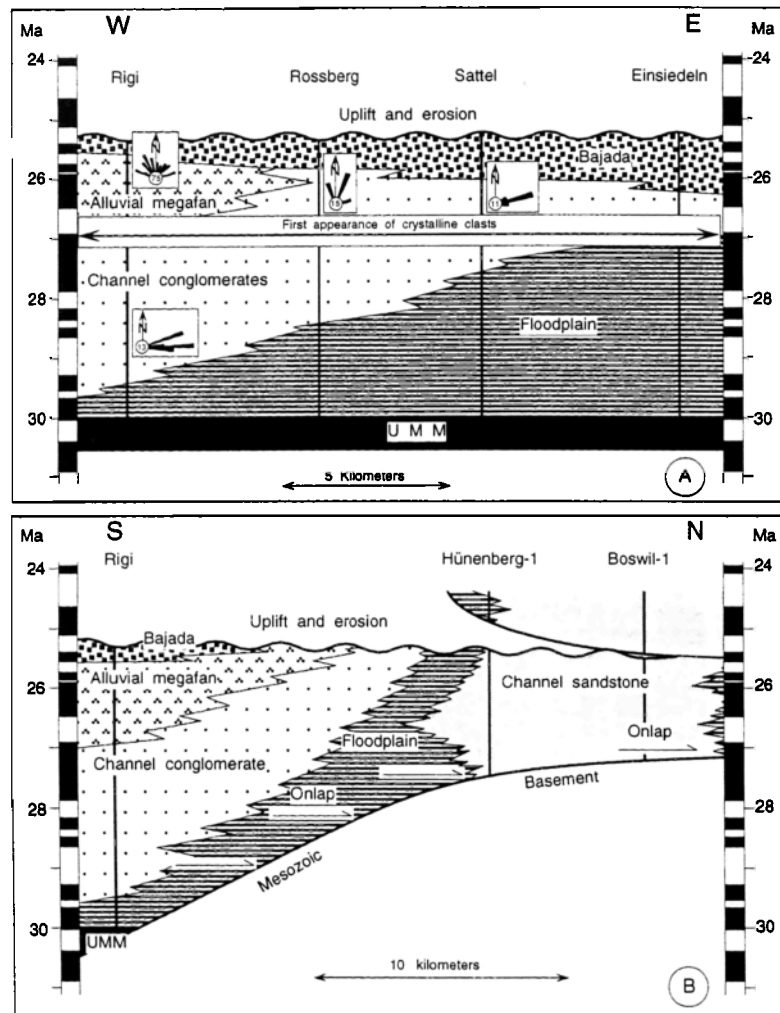
Figure 6 . (a) Wheeler diagram of the proximal basin border in a section along the thrust front, revealing strongly heterochronous facies relationships. This diagram is based on the magnetostratigraphic calibration of the Rigi section [*Schlunegger et al.,* 1997a]. The transition from the Lower Marine Molasse (UMM) to the terrestrial floodplain facies is isochronous according to *Schlunegger et al.* [1996, 1997a]. However, except for the Rigi section no chronology is available to temporally calibrate the first appearance of crystalline clasts. Nevertheless, this petrographic change is likely to be isochronous between Rigi and Einsiedeln given the short distance of ~15 km. (b) Wheeler diagram of the Oligocene central Swiss Molasse Basin, showing the temporal relationships between the proximal and the distal depositional systems (modified after *Schlunegger et al.* [1997a and b]).

mity between the Molasse deposits and the Mesozoic basement measured ≤3.5°. At ~27 Ma, accumulation of sediment started at Hünenberg-1 and Boswil-1 almost contemporaneously (Figure 6b). This implies that, at ~27 Ma, the angle of onlap between the foreland deposits and the Mesozoic carbonates decreased significantly to ≤1.5° (Figure 7).

3.3. Interpretation

The continuous subsidence at Rigi between 30 and 25 Ma is interpreted to have been caused by crustal loading by forward thrusting of the frontal Alpine nappes. Indeed, relationships between temporally calibrated metamorphic fabrics and struc-

tures [*Frey et al.,* 1980a, b; *Erdelbrock,* 1994; *Rahn et al.,* 1994, 1995] indicate that forward thrusting of the Helvetic units and the piggyback stack of Penninic and Austroalpine nappes occurred along the basal Alpine thrust between ~30 and 25 Ma (Calanda phase of deformation [*Milnes and Pfiffner,* 1977, 1980]). Furthermore, to explain the increase of the sediment-accumulation rate at Rigi at ~27 Ma, we interpret that at that time, the rate of crustal loading at the Alpine thrust front increased, resulting in enhanced basement deflection and hence an increase of the sediment accumulation rates [e.g., *Flemings and Jordan,* 1989, 1990]. Enhanced crustal thickening at the thrust front is likely to have increased the topographic gradient, which in turn would promote enhanced erosional
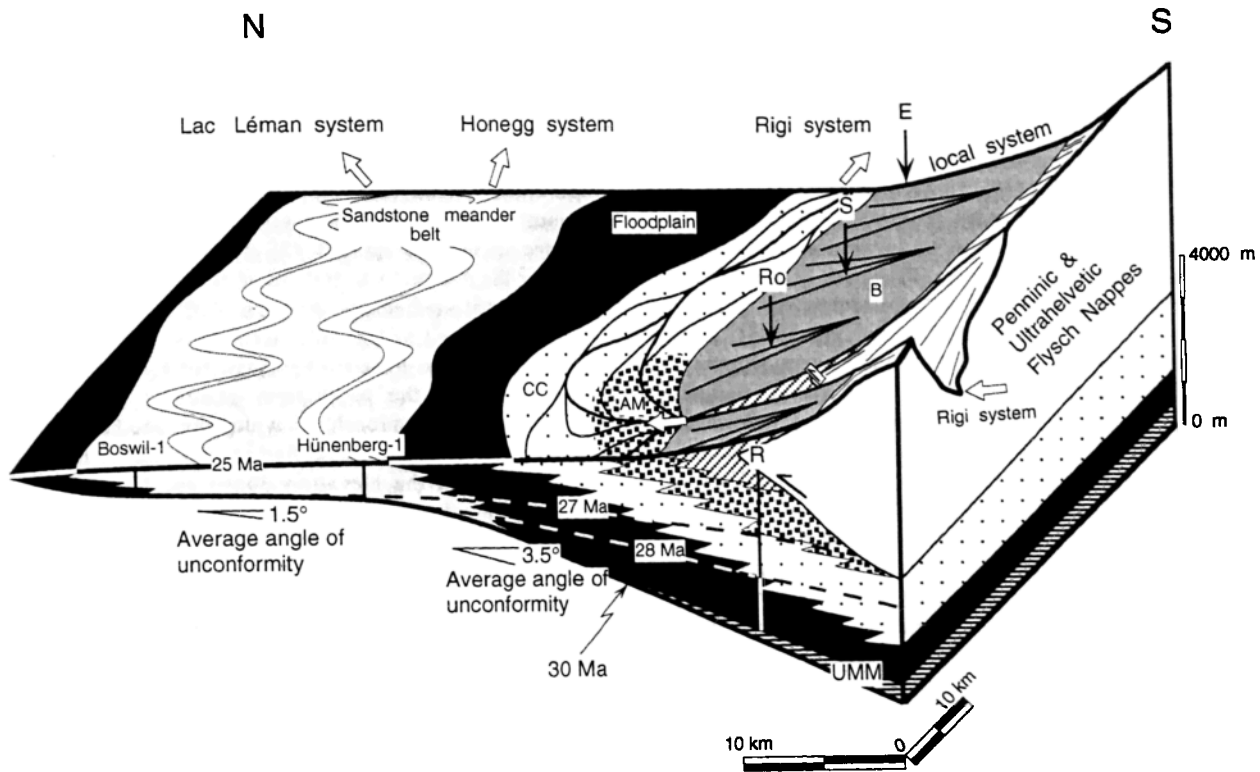
Figure 7. Three-dimensional reconstruction of the architecture of the 25-Ma Molasse Basin. Depositional systems: AM, alluvial megafan; B, bajada; and CC, conglomerate channel belt. Stratigraphic sections: R, Rigi section; Ro, Rossberg section; S, Sattel; and E, Einsiedeln.

denudation of the frontal Alpine units and thus explain the presence of locally sourced bajada fans at the top of the sections bordering the frontal Alpine nappes [e.g., *Paola et al.*, 1992] (Figure 7).

Using diffusion models of mountain belt uplift and erosion, *Flemings and Jordan* [1989, 1990], *Sinclair et al.* [1991], and *Paola et al.* [1992] tested the consequence of enhanced crustal loading in the frontal part of an orogen in which all other variables remain constant. They concluded that this situation causes an increase of the accommodation space/sediment supply ratio in the foreland basin. As a result, the facies boundaries retreat with respect to the thrust front. The stratigraphic data of the Molasse Basin, however, suggest that the time period of enhanced crustal loading at the thrust front (27-25 Ma) is associated with an increase of the progradation rate of the Rigi fan, expansion of the width of the basin, and a decrease of the angle of unconformity between the Molasse deposits and the Mesozoic basement. This implies that the sediment supply of the major contributors of sediment to the study area (Rigi and Lake Thun rivers [*Schlunegger et al.*, 1997b]) must also have increased significantly at ~27 Ma. Indeed, metamorphic and cooling ages suggest that in the source terrain of the Rigi river, maximum exhumation rates occurred between 32±5 Ma and 25±2 Ma (Figure 4). In the hinterland of the Lake Thun river, maximum erosion rates appear to have occurred between 27±5 Ma and 22±2 Ma at an average rate that was ~50% higher than the one determined for the source area of the Rigi river

(Figure 4). This implies that (1) the total supply of sediment to the study area increased between 30 and 20 Ma and (2) an enhanced increase of the average supply rate of sediment is likely to have occurred at ~27 Ma.

4. Palinspastic Restoration of the Orogenic and Sedimentary Load at 25 Ma

4.1. Methods

In order to calculate the curvature of the foreland plate at 25 Ma and thereby estimate the strength of the lithosphere during formation of the foreland basin, it is necessary to restore the orogenic load for that time. In this paper, we used the tectonostratigraphic balanced cross section of *Schmid et al.* [1996] (Figure 1b). Despite its oblique orientation with respect to the Alpine strike and despite the rather large distance to the study area (~50 km), we justify the usage of this section because (1) it partly covers the source area of the Rigi river (Figure 1a), (2) its tectonic architecture and structural evolution are reasonably well known [*Schmid et al.*, 1996], and (3) the mechanical structure for this part of the Alps has recently been explored [*Okaya et al.*, 1996a].

At 25 Ma, the Penninic, Austrolapine and Helvetic nappes had already been emplaced [*Milnes and Pfiffner*, 1977, 1980; *Burkhard*, 1988], and the Insubric phase of back thrusting in

southeastern Switzerland with a vertical displacement of >10 km as well as the intrusion of the Bergell pluton were almost completed [*Gulson*, 1973; *Koeppel and Grünenfelder*, 1975; *Hurford*, 1986; *Schmid et al.*, 1989]. Following *Schmid et al.* [1996], we restored a total of ~85 km of relative movements between the European and Adriatic plates, which compose ~35 km of shortening north of the Insubric Line, and ~50 km of shortening in the Southern Alps [*Schönborn*, 1992] that are, however, badly constrained due to imprecise chronological data [*Schmid et al.*, 1996, Figure 4]. North of the Insubric Line, we restored (1) 6 km of shortening for the Jura Mountains of eastern Switzerland [*Naef et al.*, 1985], (2) 24 km for the Subalpine Molasse/Aar massif system [*Pfiffner et al.*, 1996; *Schlunegger et al.*, 1997a], (3) 5 km of shortening for the Helvetic thrust nappes (Ruchi phase of deformation [*Milnes and Pfiffner*, 1977, 1980; *Erdelbrock*, 1994; *Rahn et al.*, 1995; *Wang et al.*, 1995]) that is interpreted as gravitational collapse [*Menkveld*, 1995], and (4) <1 km of shortening for the sinistral transpressional movements along the Engadine Line [*Schmid and Froitzheim*, 1994]. In this restoration, east directed extensional features in the Penninic nappes (Forcola phase of deformation [*Schmid et al.*, 1996]) as well as small-scale compressional structures in the Penninic thrust nappes (e.g., crenulation fabrics) are discarded. This is justi-

fied because the contribution of these structures to the total amount of shortening is negligible [*Schmid et al.*, 1996].

In addition to these restored offsets (Figure 8a), the load of the Alpine orogen added onto the foreland plate at ~25 Ma (Figure 8c) must include material lost by exhumation. This was determined by calculating the overburden of the tectonostratigraphic units using (1) temporally and thermally calibrated metamorphic mineral parageneses and cooling ages for the Alps (see the next paragraph), (2) an average density of 2700 kg/m^3 for the Alpine rocks [*Okaya et al.*, 1996a], and (3) average geothermal gradients of 20°C/km, 25°C/km, and 30°C/km that are considered to take into account the major uncertainties. Of these, large uncertainties exist for the thermochronological data and the geothermal gradients. *Soom* [1990] demonstrated one approach of evaluating geothermal gradients. He showed, using apatite fission track data, a linear relationship between the elevation above sea level where the samples were collected and the time when the samples passed through the closure temperature of apatite. Extrapolating average present-day uplift rates to the upper Miocene and using the elevation/age relationships of the apatite fission track data, *Soom* [1990] determined geothermal gradients between 25°C/km and 30°C/km. However, thermal modeling of a coalification profile in the Subalpine Molasse of central
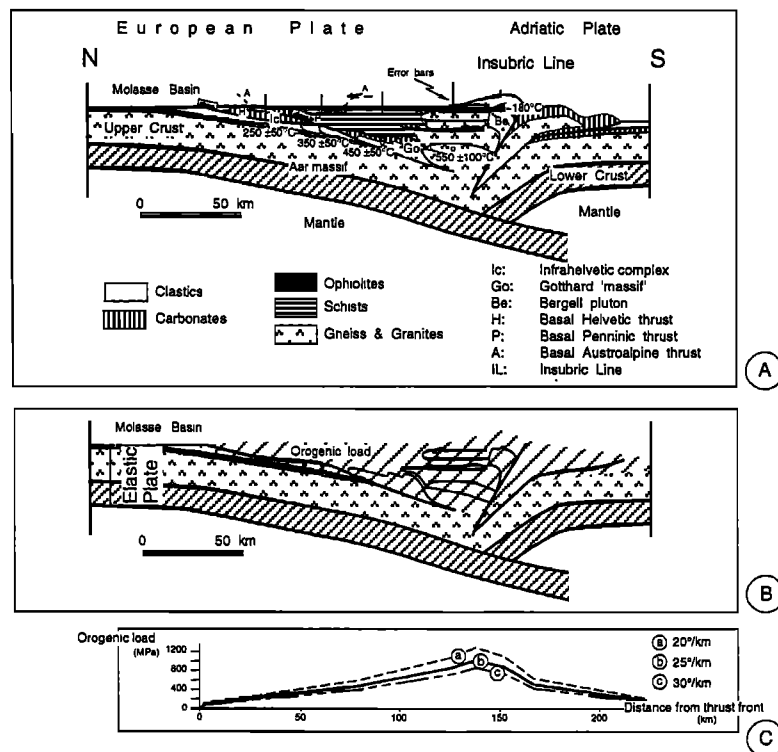

Figure 8. (a) Restored section across the 25-Ma Alps. The thickness of the Alpine edifice was calculated using average values of temporally and thermally calibrated metamorphic mineral parageneses and a geothermal gradient of 25°C/km. The error bars represent possible variations in the crustal loads due to uncertainties in the geothermal gradient (20°-30°C/km) and in the temporal and thermal calibration of the metamorphic fabrics and the closure temperatures. See text for discussion. (b) Orogenic load determined for a geothermal gradient of 25°C/km and for the average temperatures of the buried Alpine units shown on Figure 8a. (c) Effective orogenic load added onto the plate for geothermal gradients of 20°C/km, 25°C/km, and 30°C/km. Note that we used the average temperatures of the buried Alpine units at 25 Ma (Figure 8a) as reference.

Switzerland suggests that in the late Oligocene the geothermal gradient measured between 20° and 23.5°C/km [*Schegg*, 1994]. Alternatively, on the basis of the results of a thermokinematic model of the Alpine orogeny, *Okaya et al.* [1996b] concluded that in active collisional zones temperature gradients change dramatically with depth and laterally through the collision zone. Their model suggests that immediately north of the Insubric Line the present-day geothermal gradient decreases from 20°C/km in upper crustal levels to <5°C/km in the lower crust.

The average temperatures of the buried Alpine nappes at ~25 Ma are presented on Figure 8a. At that time, progressive heating to ~250°C ±50°C of the Infrahelvetic complex was completed [*Rahn et al.*, 1994; *Wang et al.*, 1995]. Also at ~25 Ma, Rb-Sr and K-Ar ages determined on biotite suggest that the central Aar massif reached temperatures of ~350°C ±50°C according to *Dempster* [1986] and *Soom* [1990]. The thermal data for the Gotthard "massif" is taken from *Steiger* [1964] and *Deutsch and Steiger* [1985]. These authors suggest that at ~25 Ma synmetamorphic growth of hornblende occurred at a temperature of ~450°C ±50°C. The thermal evolution of the Penninic nappes of the Central Alps and the Bergell pluton (Figures 1b and 8a) is presented and discussed by *Hurford* [1986], *Hurford et al.* [1989], and *Giger* [1991]. These authors suggest that at ~25 Ma the crystalline core of the Penninic nappes cooled down to ~550°C ±100°C (Figure 8a), whereas the temperature of the Bergell pluton measured ~180°C.

The sediment load of the Molasse Basin (Figure 9a) was determined using the measured thicknesses of stratigraphic sections (Figure 3a) and a density of 2400 kg/m^3 for sedimentary rocks [*Turcotte and Schubert*, 1982].

4.2. Results

The restoration of the Alpine edifice in the late Chattian is presented on Figure 8a. Despite the uncertainties that arise from the poorly constrained geothermal gradient and from the rather large error bars in the temporal and thermal calibration of the metamorphic fabrics and the closure temperatures, our restoration reveals that the Austroalpine nappes, which formed the orogenic lid, were almost completely eroded at that time. Furthermore, according to Figure 8a the Helvetic thrust nappes were not exposed to erosion at 25 Ma. These findings are consistent with petrographic data collected from the Molasse Basin of central Switzerland, which indicate that (1) the clasts derived from Austroalpine nappes disappear at ~24 Ma in the study area [*Tanner*, 1944; *Speck*, 1953; *Schlunegger et al.*, 1996a], and (2) erosion of the Helvetic thrust nappes started at ~15 Ma [*Matter*, 1964]. Furthermore, Figure 8b and Figure 8c show that the tectonic load in the northern and southern orogen increases from the proximal border of the northern and southern forelands to the Penninic crystalline nappes, where highest crustal loads of ~1200 MPa were present.

5. Modeling of the Foreland Basin Deflection

Regional isostatic compensation is the prinicipal driving force of the subsidence in foreland basins, as the lithosphere accommodates the loading by flexure [*Watts and Ryan*, 1976; *Jordan*, 1981; *Beaumont*, 1981; *Flemings and Jordan*, 1989; *Sinclair et al.*, 1991; *Jordan*, 1995]. The deflection of a plate

due to an applied load is a function of (1) the continuity of the plate, (2) the rheological properties of the plate (elastic vs. viscoelastic), (3) the distribution and magnitude of the load, and (4) the mechanical properties of the plate, expressed by the flexural rigidity [*Hetényi*, 1946; *Turcotte and Schubert*, 1982; *Flemings and Jordan*, 1989; *Peper*, 1993; *Johnson and Beaumont*, 1995; *Okaya et al.*, 1996b].

A first evaluation of the mechanical properties of the north Alpine foreland plate was performed by *Karner and Watts* [1983] using gravity anomalies. These authors estimated an elastic thickness (*Te* value) between 20 and 50 km for the plate underlying the Alps. A more detailed study was carried out by *Lyon-Caen and Molnar* [1989]. These authors modeled the present-day Bouger gravity anomalies for four sections across the Alps and the Molasse Basin. They revealed that the measured complete Bouger gravity anomalies over the core of the present-day Alps are similar to those calculated assuming local isostatic equilibrium but are makedly out of isostatic equilibrium in the areas surrounding the Alps, for example, the Molasse Basin. The Bouger gravity anomalies of this basin was most successfully simulated by these authors for a weak plate with an elastic thickness of ~15 km. However, such a weak elastic plate does not account for the excess of mass in the Vosges and the Black Forest (Figure 1a). On the basis of these findings, *Lyon-Caen and Molnar* [1989] concluded that gravity anomalies do not place a useful constraint on the flexural rigidity of the plate or on the forces that formed the Molasse Basin.

A careful assessment of the mechanical properties of the north Alpine foreland plate at 17 Ma was carried out by *Sinclair et al.* [1991]. These authors determined the mechanical properties of the plate by simulating the deflection of the basement, using a constant taper of 28° for the Alpine orogenic wedge [*Pfiffner*, 1986] and a broken plate model. They changed the elastic thickness of the plate (*Te* value) and the width of the orogenic load iteratively until they reached a best fit simulation of the foreland plate deflection. They concluded that, at 17 Ma, the elastic thickness of the foreland plate measured 10±5 km and that the deflection of the basement was controlled by a 100-km-wide thrust belt. Because *Sinclair et al.* [1991] iteratively changed the tectonic load and the elastic thickness of the plate as well, their determination of the mechanical properties of the foreland plate is nonunique. Nevertheless, these authors stated that it would be difficult to use a *Te* value that was much greater than 15 km if parameters were kept within reasonable bounds.

Using gravity data, the curvature of the basement between the featheredge of the Molasse Basin and the thrust front, and a broken plate model, *Royden* [1993] determined an elastic thickness of ~50 km for the north Alpine foreland plate. Following Royden, the deflection of the present-day basement beneath the Alps and the Molasse Basin is controlled by the orogenic load with contributions of a vertical shear force and a bending moment exerted at the end of the plate. The model of Royden, however, fails to explain the steep curvature of the plate beneath the Molasse Basin and the limited width of this basin [e.g., *Sinclair et al.*, 1991].

The most recent estimate of the present-day flexural rigidity of the European plate was published by *Okaya et al.* [1996b]. These authors determined the mechanical structure of the lithosphere through the Alpine collision by calculating strength
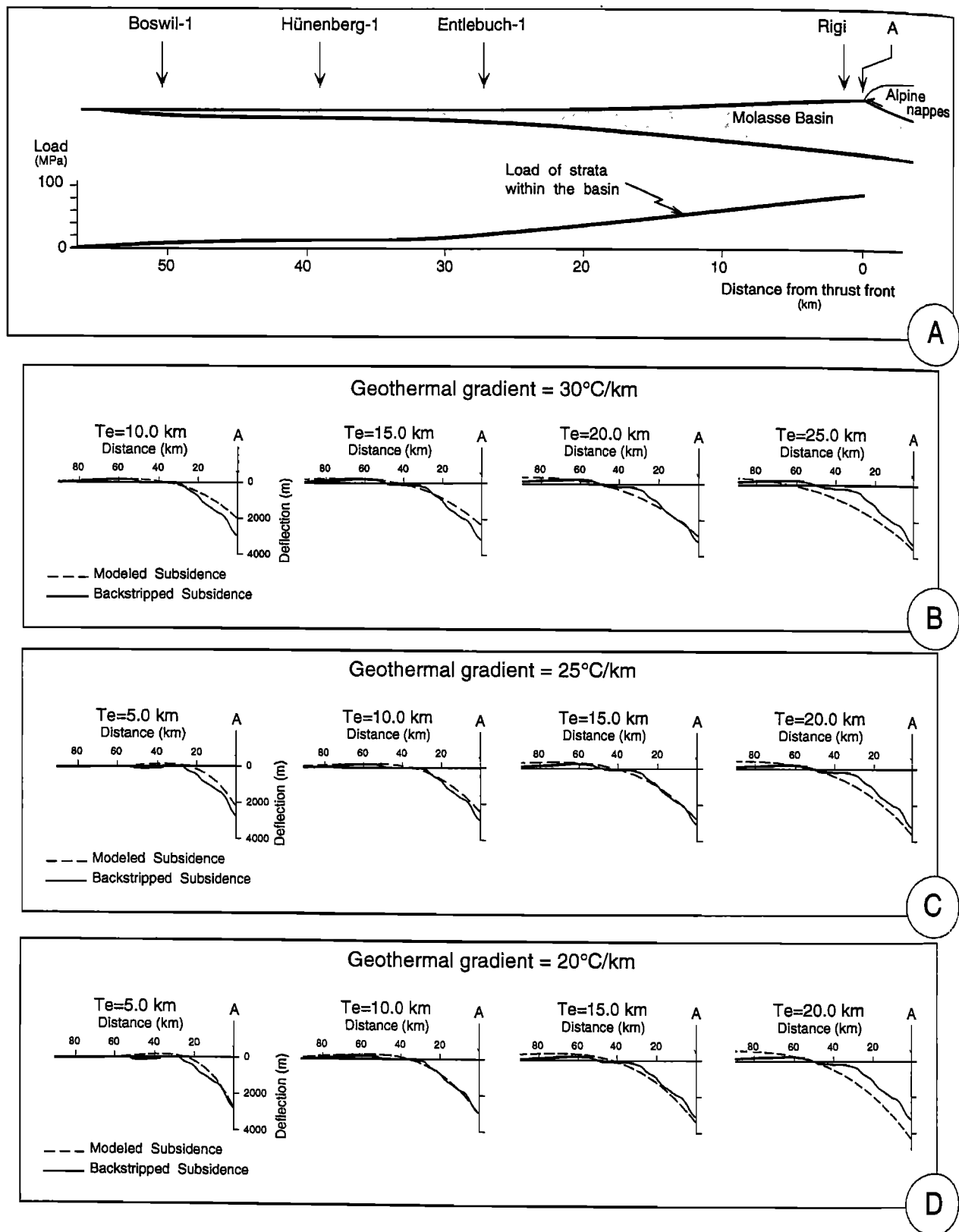
Figure 9. (a) Crustal loads exerted by the sediments of the Molasse Basin. The magnitude of these loads was determined using the thickness of strata (Figure 3a) and a density of 2400 kg/m³. (b) to (d) Model results, revealing the profiles of the north Alpine foreland plate determined for different Te values and geothermal gradients of (b) 30°/km, (c) 25°C/km, and (d) 20°C/km. The tectonic subsidence was determined by back stripping. See text for further explanation.

envelopes across the orogen. This was performed by considering depth profiles of lithospheric material, rheology, strain rate, and temperature that was gained from thermokinematic modeling [Okaya et al., 1996a]. Okaya et al. determined Te values for the north Alpine foreland plate that scatter between ~25 and 40 km dependent on whether they used a broken or a continuous plate or whether they assumed that the crust and the mantle are mechanically coupled or decoupled.

In this paper, we used a model for a continuous elastic beam overlying a fluid substratum, the cross-sectional geometry of the Molasse Basin (Figure 3a), the distributed load of the Alps at ~25 Ma (Figure 8c), and the numerical solutions given by Hetényi [1946] and Jordan [1981] to simulate the tectonic subsidence of the Molasse Basin and thereby assess the mechanical properties of the north Alpine foreland plate. We justify the usage of a continuous rather than a broken plate model because seismic, structural, geochronological, and stratigraphical data indicate that insertion of the Adriatic lower crust into the interface between the south dipping European lower crust and the European upper crust started in the Late Cretacous [Schmid et al., 1996; Lihou and Allen, 1996], which in turn suggests that the European and Adriatic plates behaved with continuous rather than broken plate conditions since late Oligocene at the latest (Figure 8a). Indeed, any vertical movement of the European plate had to be accommodated by deflection of the Adriatic plate or plastic flow of rocks in order to keep a volumetrical balance. The identation of the two plates implies that, although the paleogeographically distinct European plate is discontinuous and broken and although the European and Adriatic plates are likely to have different flexural strenghts [Royden, 1993; Okaya et al., 1996b], the mechanical as well as the rheological unit was continuous beneath the Alps during the "Molasse" stage of the basin evolution. Furthermore, because sediment-accumulation rates and admixture and size of clasts derived from the frontal thrusts increased simultaneously (see above), we interpret that the foreland plate reacted instantaneously to crustal loading events. This implies that elasticity represents a reasonable boundary condition for modeling the deflection of the Molasse Basin [see also Turcotte and Schubert, 1982]. Finally, we justify the usage of the cross-sectional geometry of the Molasse Basin as principal constraints for our model because Sinclair et al. [1991] and Sinclair [1996] argued successfully that the cross-sectional as well as the plan view geometry of the Molasse Basin provide the most detailed and the most decipherable information about possible controls on the forces that caused the plate beneath the Molasse Basin to flex.

To identify the probable elastic thickness at 25 Ma, we compare the results of forward and inverse (back stripping) models for which the Te value is the unknown. The tectonic subsidence of the Molasse Basin was determined by back stripping of the sediment load (Figures 9a to 9d). These results for the Molasse Basin were then compared with the forward modeled deflection of the foreland plate (Figure 9b) that was calculated using the distributed orogenic load shown in Figure 8c. Both the back stripping and the forward modeling were iterated through Te values. We divided the orogenic load (Figure 8c) and the sediment load (Figure 9a) into 2.5-km-wide segments before performing the numerical calculations.

The results of the flexural modeling reveal that a successful simulation of the deflection of the plate is dependent on the

magnitude of the applied load and the effective elastic thickness of the plate. Low crustal loads that were obtained for a geothermal gradient of 30°C/km fail to explain the high slope of the basement adjacent to the thrust front (Figure 9b). Good fits between the back stripped subsidence and the modeled subsidence are achieved for (1) higher crustal loads that were determined for geothermal gradients of 20°C/km and 25°C/km and (2) very low Te values between 10 and 15 km (Figures 9c and 9d). This implies that the European foreland plate was weak during deposition of the Lower Freshwater Molasse group. An elastic thickness of ~10-15 km, which was determined by including the Alpine orogenic load and the sediment load of the basin, is consistent with the low Te values of 10±5 km determined by Sinclair et al. [1991].

Despite the successful simulation of the deflection of the 25-m.y.-old Molasse Basin, the presented model has several drawbacks: (1) crustal heterogeneities such as reactivated normal faults as well as thermal and density anomalies [Rey et al., 1990; Laubscher, 1990; Stäuble and Pfiffner, 1991; Okaya et al., 1996a] were discarded in the model, which, however, might change the elastic property of the crust [Washbusch and Royden, 1992; Okaya et al., 1996b], (2) the assumption that the mechanical properties of the Adriatic plate are the same as those of the European plate might be incorrect [Royden, 1993; Okaya et al., 1996a], (3) possible three-dimensional heterogeneities in the orogenic load are discarded in our model, and (4) major uncertainties arise from underestimates or overestimates of the orogenic load (see section 4). Nevertheless, our model supports the findings of Lyon-Caen and Molnar [1989] and Sinclair et al. [1991] that the strength of the European lithosphere is possibly very low beneath the Molasse Basin or even zero beneath the roots of the Alps. If these conclusions are correct, then differences in the flexural strength between the European and Adriatic plates has an insignificant influence on the forces that caused the Molasse Basin to subside [Sinclair et al., 1991]. Furthermore, using a weak foreland plate, we can explain (1) the high angle of deflection of the plate beneath the Molasse Basin (Figure 3a), (2) the narrow width of the basin, and (3) the small radius of the plan view curvature of the Molasse Basin southwest of the study area [Sinclair, 1996].

6. Discussion and Conclusion

The deflection of the central Swiss Molasse basin at 25 Ma is the net result of the deflection due to the orogenic load and due to the load of the basin fill (Figure 10). These two components, however, are of significantly different wavelengths and amplitudes. Whereas the orogenic load causes a narrow, deep, strongly curved foreland basin, the sedimentary load of the basin tends to smooth the deflection of the foreland plate. Furthermore, Figure 10 reveals that >60% of the total accommodation space of the basin was formed by deflection due to the sediment load.

The calculated model clearly reveals that the Lac Léman and Honegg dispersal systems are located on what would have been a forebulge in a basin with no sediment accumulation (Figure 10). The hypothesis of the presence of a tectonically driven forebulge in this area as suggested by the numerical model is supported by the decrease of the angle of unconformity south of Hünenberg-1 (Figure 5) [see also Crampton and Allen,
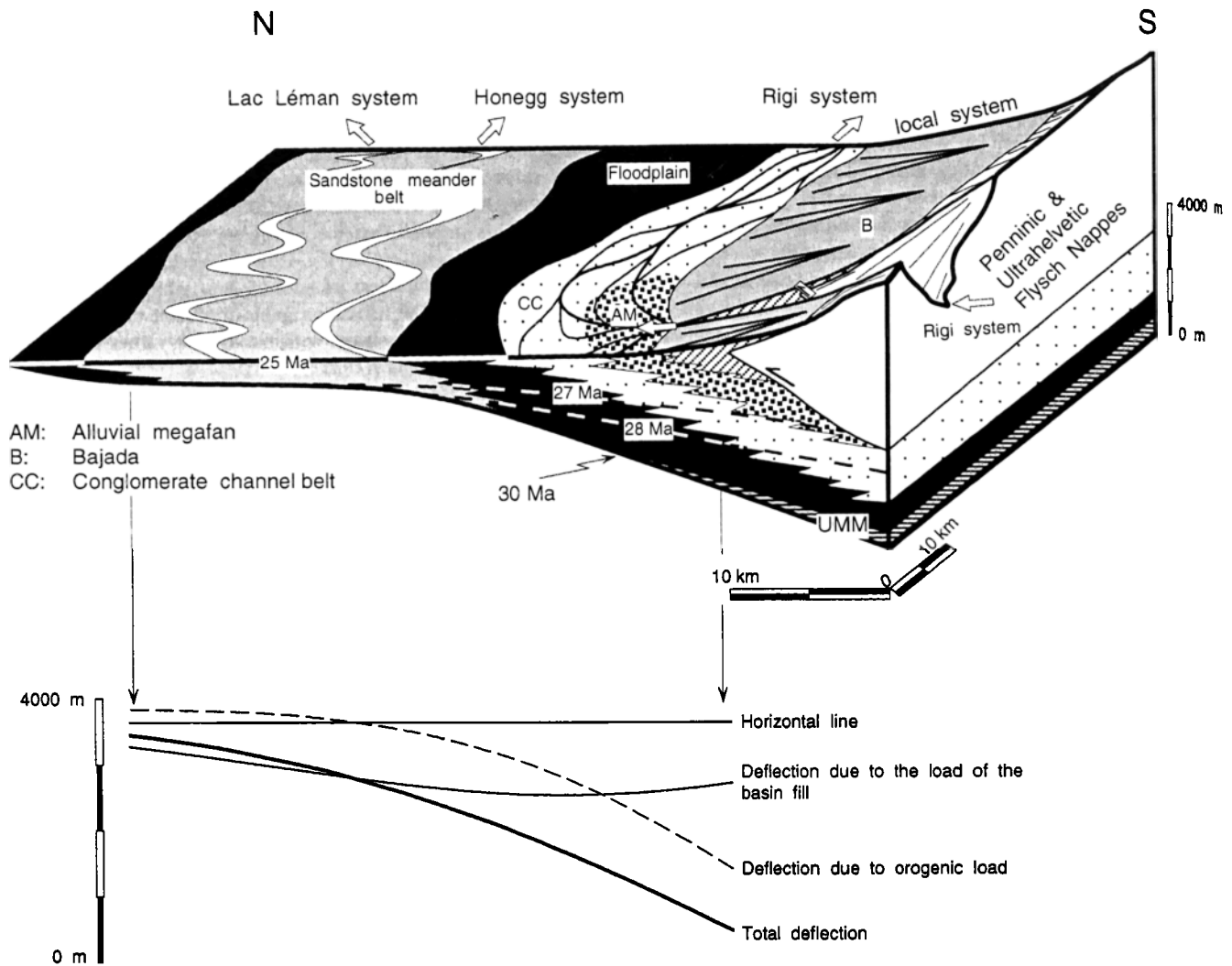
Figure 10. Model results for Te=10 km and a geothermal gradient of 25°C/km, revealing that 60% of the total deflection of the Molasse Basin is due to the sediment load. The model reveals that the Lac Léman and Honegg dispersal systems are located on a buried flexural bulge.

1995]. The net subsidence of this part of the basin is the sum of a negative and a positive component. Whereas the orogenic load caused forebulge uplift, the sedimentary fill of the basin initiated subsidence of the orogenically driven forebulge. Because of the double control of subsidence as outlined above, enhanced crustal loading in the hinterland at a constant sediment supply rate tends to promote uplift in the northern depositional domain and to create a forebulge unconformity, resulting in underfilling of the foreland basin [see *Jordan*, 1995]. If instead sediment supply increases while thrust rate is constant, the result is suppression and burial of the forebulge and overfilling of the basin [*Flemings and Jordan*, 1989, 1990; *Sinclair et al.*, 1991; *Jordan*, 1995; *Crampton and Allen*, 1995]. According to the model of *Crampton and Allen* [1995] the Oligocene deposits of central Switzerland are likely to represent the transition from the underfilled to the overfilled stage of the basin. Northward onlap of 30-to 28-Ma deposits on the

Mesozoic basement suggests the presence of a forebulge unconformity (underfilled stage), whereas burial of the teconically driven forebulge by the 27 to 25 Ma strata indicates overfilling of the basin.

The increase of the sediment accumulation rates from initally 700 m/m.y. to >1000 m/m.y. at Rigi, which occurred simultaneously with the 27 Ma geometry transition, suggests enhanced orogenic loading from frontal propagation and stacking [*Schlunegger et al.*, 1997a]. The coincidence of overfilling with enhanced crustal loading in the orogen implies that the sediment supply rate to the foreland basin increased simultaneously. Indeed, cooling ages from the source area of the Rigi river indicate, as discussed above, enhanced exhumation of the Central Alps of eastern Switzerland between ~30 and 25 Ma (Figure 4). It appears therefore that enhanced erosional denudation in this part of the Alps caused an augmentation of the sediment supply by the Rigi river, which increased

the sedimentary load in the basin. As a result, subsidence in the northern domain was initiated, and the wavelength of the basin increased (Figure 10).

Whereas the subsidence driven by the tectonic load tends to concentrate the dispersal systems at the thrust front, the subsidence due to the sediment load favors migration of the drainage axis to the central part of the basin [Flemings and Jordan, 1989, 1990]. This implies that, if sediment supply to the foreland basin increases at a constant thrust rate, the location of maximum deflection driven by the sediment load shifts away from the thrust front. As a result, the subsidence rates increase in the center of the basin with respect to those at the thrust front. This change in the basin subsidence configuration causes fan progradation and fanhead entrenchment. If, however, thrust rates decrease and supply of sediment to the basin increases, erosion might occur in the proximal part of the foreland basin. We interpret that the erosional event in the proximal Molasse Basin and the northward shift of the depocenters of the depositional systems at the Oligocene/Miocene boundary (Figure 6b) are results of an increase in the supply rate of sediment to the distal axial drainage and a decrease of crustal loading at the thrust front. Indeed, whereas erosional denudation rates were constant in the Central Alps of eastern Switzerland at the Oligocene/Miocene boundary (Figure 4), they increased in the Central Alps of western Switzerland. This latter part of the orogen, however, was the source terrain of the distal axial dispersal systems (see discussion in section 2). Furthermore, the rate of crustal thickening due to slip movement along the basal Alpine thrust decreased nearly to zero at the Oligocene/Miocene boundary,

according to crosscutting relationships of temporally calibrated metamorphic fabrics [Schmid et al., 1996]. It appears therefore that cessation of slip movement along the basal Alpine thrust and enhanced sediment sediment supply to the distal axial drainage caused uplift and erosion of the proximal basin and a basinward shift of the axial depocenters.

Given the flexural rigidity of the plate, one can critically evaluate the importance of specific Alpine tectonic events (e.g., loading in Southern Alps versus Northern Alps) on the geometrical evolution of the north Alpine foreland basin (Figure 11). For instance, load segment 1, located in the area of the Aar massif at ~60 km distance from the thrust front, causes flexural uplift at the thrust front (Rigi section) for a Te value of 5 km. The same crustal load, however, causes flexural downwarp at Rigi for a Te value ≥ 10 km. Load segment 2, located in the area of the Gotthard "massif" at 100 km distance from the thrust front, has zero influence on the deflection at Rigi for a Te value of 5 km. For an elastic thickness of 10 km, the same load causes uplift at Rigi, whereas it causes flexural downwarp at the same locality for Te values ≥ 20 km (Figure 11). Since at 25 Ma the elastic thickness of the north Alpine foreland plate measured ~10 km, the width of the orogen that caused flexural downwarp at the thrust front measured ~70 km. Orogenic loads beyond this area, that is, the Gotthard "massif" and the piggyback stack of Penninic nappes, either caused flexural uplift of the proximal basin border or had zero influence on the deflection at the thrust front. This implies that, although the Central Alps north of the Insubric Line exerted the greatest load onto the foreland plate at 25 Ma (Figure 8c), they did not significantly affect the tectonic subsidence pattern and
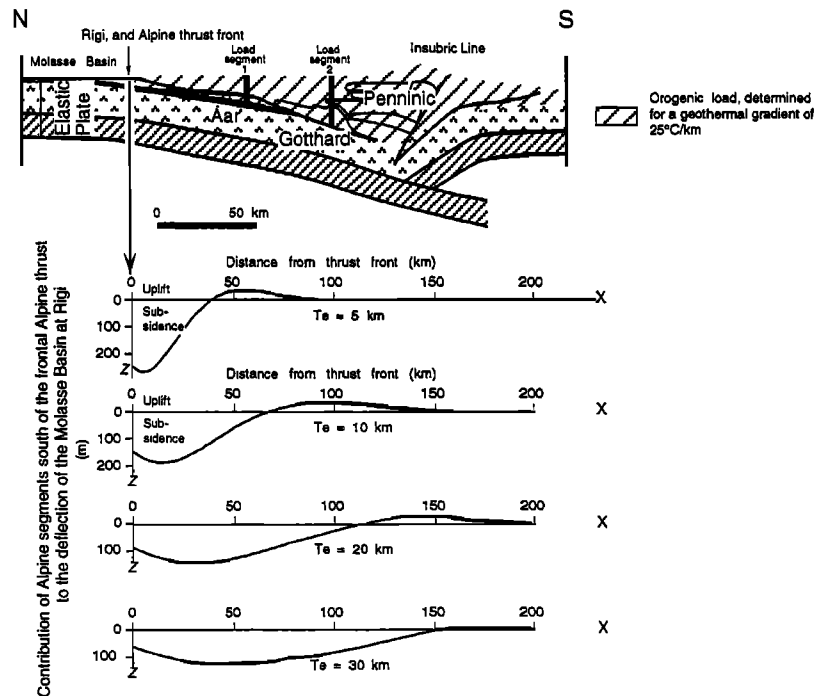

Figure 11. Model results, revealing the contribution of Alpine segments to the deflection at Rigi for different flexural rigidities of the plate. See text for detailed description.

838 SCHLUNEGGER ET AL.: MOLASSE BASIN AND ALPINE DENUDATION

the geometrical evolution of the Molasse Basin (Figure 11). However, given that denudation of the Central Alps was controlled by activity along the Insubric Line, one could conclude that there is an indirect tie between back thrusting along the Insubric Line and the geometrical evolution of the north Alpine foreland basin. Specifically, the crystalline core of the Central Alps was a major sediment source area.

References

Beaumont, C., Foreland basins, *Geophys. J. R. Astron., Soc., 65,* 291-329, 1981.

Berli, S., Die Geologie des Sommersberges (Kantone St. Gallen und Appenzell), *Ber. St. Gal. Natf. Ges., 82,* 112-145, 1985.

Burkhard, M., L'Hélvetique de la bordure occidentale du massif de l'Aar (évolution tectonique et métamorphique), *Eclogae Geol. Helv., 81,* 63-114, 1988.

Buxtorf, A., T. Tobler, G. Niethammer, E. Baumberger, P. Arbenz, and W. Staub, Geologische Vierwaldstätterseekarte, scale 1:50000 (Spezialkarte 66a), Schweiz. Geol. Komm., Basel, 1916.

Crampton, S.L., and P.A. Allen, Recognition of forebulge unconformities associated with early stage foreland basin development Example from the north Alpine foreland basin, *AAPG Bull., 79,* 1495-1514, 1995.

DeCelles, P.G., and G. Mitra, History of the Sevier orogenic wedge in terms of critical taper wedge models, northeast Utah and southwest Wyoming, *Geol. Soc. Am. Bull., 107,* 454-462, 1995.

Dempster, T.J., Isotope systematics in minerals: Biotite rejuvenation and exchange during Alpine metamorphism, *Earth Planet. Sci. Lett., 78,* 355-367, 1986.

Deutsch, A., and H. Steiger, Hornblende K-Ar ages and the climax of Tertiary metamorphism in the Lepontine Alps (south-central Switzerland): An old problem reassessed, *Earth Planet. Sci. Lett., 72,* 175-189, 1985.

Diem, B., Die Untere Meeresmolasse zwischen der Saane (Westschweiz) und der Ammer (Oberbayern), *Eclogae Geol. Helv., 79,* 493-559, 1986.

Engi, M., S.C. Todd, and D.R. Schmatz, Tertiary metamorphic conditions in the eastern Lepontine Alps, *Schweiz. Mineral. Petrogr. Mitt., 75,* 347-396, 1995.

Erdelbrock, K., Diagenese und schwache Metamorphose im Helvetikum der Ostschweiz 'Inkohlung und Illit-'Kristallinität', Ph.D. thesis, 220 pp., Univ. of Aachen, Aachen, Germany, 1994.

Flemings, P.B., and T.E. Jordan, A synthetic stratigraphic model of foreland basin development, *J. Geophys. Res., 94,* 3851-3866, 1989.

Flemings, P.B., and T.E. Jordan, Stratigraphic modelling of foreland basins: Interpreting thrust deformation and lithospheric rheology, *Geology, 18,* 430-434, 1990.

Frey, M., K. Bucher, E. Frank, and J. Mullis, Alpine metamorphism along the Geotraverse Basel-Chaisso - a review, *Eclogae Geol. Helv., 73,* 527-546, 1980a.

Frey, M., M. Teichmüller, R. Teichmüller, J. Mullis, B. Künzi, A. Breitschmid, U. Grunder, and B. Schwizer, Very low-grade metamorphism in the external parts of the Central Alps: illite crystallinity, coal rank and fluid inclusion data, *Eclogae Geol. Helv., 73,* 173-203, 1980b.

Füchtbauer, H., Die Schüttungen im Chatt und Aquitan der deutschen Alpenvorlandmolasse, *Eclogae Geol. Helv., 51,* 928-941, 1959.

Füchtbauer, H., Sedimentpetrographische Untersuchungen in der älteren Molasse nördlich der Alpen, *Eclogae Geol. Helv., 61,* 157-298, 1964.

Gasser, U., Die innere Zone der subalpinen Molasse des Entlebuchs (Kt. Luzern), Geologie und Sedimentologie, *Eclogae Geol. Helv., 61,* 229-313, 1968.

Giger, M., Geochronologische und petrographische Studien an Geröllen und Sedimenten der Gonfolite Lambarda Gruppe (Südschweiz und Norditalien) und ihr Vergleich mit dem alpinen Hinterland, Ph.D. thesis, 227 pp., Univ. of Bern, Bern, 1991.

Gulson, B. L., Age relations in the Bergell region of the southeast Swiss Alps, with some geochemical comparisons, *Eclogae Geol. Helv., 66,* 293-314, 1973.

Hetényi, M., *Beams on Elastic Foundation,* 255 pp., Univ. of Mich. Press, Ann Arbor, 1946.

Homewood, P., P.A. Allen, and G.D. Williams, Dynamics of the Molasse Basin of western Switzerland, in *Foreland Basins,* edited by P.A. Allen and P. Homewood, *Spec. Publ. Int. Assoc. Sedimentol., 8,* 199-217, 1986.

Hunziker, J.C., J. Desmons, and A.J. Hurford, Thirty-two years of geochronological work in the central and western Alps; a review of seven maps, *Mem. Geol. Lausanne, 13,* 59 pp., 1992.

Hurford, A.J., Cooling and uplift patterns in the Lepontine Alps south central Switzerland and an age of vertical movement on the Insubric fault line, *Contrib. Mineral. Petrol., 93,* 413-427, 1986.

Hurford, A.J., Uplift and cooling pathways derived from fission track analysis and mica dating: A review, *Geol. Rundsch., 80,* 349-368, 1991.

Hurford, A.J., M. Flysch, and E. Jäger, Unraveling the thermo-tectonic evolution of the Alps: A contribution from fission track analysis and mica dating, in *Alpine Tectonics,* edited by M. Coward et al., *Geol. Soc. Spec. Publ., 45,* 298-369, 1989.

Humi, A., Geologie und Hydrogeologie des Truebtales, Master's thesis, 153 pp., Univ. of Bern, Bern, 1991.

Jäger, E., E. Niggli, and E. Wenk, Rb-Sr Altersbestimmungen an Glimmern der Zentralalpen, *Beitr. Geol. Karte Schweiz, 134,* 67 pp., 1967.

Johnson, D.D., and C. Beaumont, Premlimianary results from a planform kinematic model of orogen evolution, surface processes and the development of clastic foreland basin stragraphy, in *Stratigraphic Evolution of Foreland Basins,* edited by S.L. Dorobek and G.M. Ross, *Spec. Publ. Soc. Econ. Paleontol. Mineral., 52,* 3-24, 1995.

Jordan, T.E., Thrust loads and foreland basin evolution, Cretaceous, western United States, *AAPG Bull., 65,* 2506-2520, 1981.

Jordan, T.E., Retroarc foreland and related basins, in *Tectonics of Sedimentary Basins,* edited by R.V. Ingersoll and K. Busby, pp. 331-362, Blackwell Sci., Cambridge, Mass., 1995.

Jordan, T.E., and P.B. Flemings, Large-scale stratigraphic architecture, eustatic variation, and unsteady tectonism: A theoretical evaluation, *J. Geophys. Res., 96,* 6681-6699, 1991.

Karner, G.D., and A.B. Watts, Gravity anomalies and flexure of the lithosphere at mountain ranges, *J. Geophys. Res., 88,* 10477-10499, 1983.

Keller, B., Fazies und Stratigraphie der Oberen Meeresmolasse (Unteres Miozän) zwischen Napf und Bodensee, Ph.D. thesis, 277 pp., Univ. of Bern, Bern, 1989.

Koeppel, V., and M. Grünenfelder, Concordant U-Pb ages of monazite and xenotime from the Central Alps and the high-temperature Alpine metamorphism, a preliminary report, *Schweiz. Mineral. Petrogr. Mitt., 55,* 129-132, 1975.

Laubscher, H.P., Deep seismic data from the central Alps: Mass distributions and their kinematics, in *Deep structure of the Alps,* edited by F. Roure et al., *Mém. Soc. Géol. France, 156,* 335-343, 1990.

Lihou, J.C., and P.A. Allen, Importance of in-

herited rift margin structures in the early North Alpine Foreland Basin, Switzerland, *Basin Res.*, 8, 425-442, 1996.

Lyon-Caen, H., and P. Molnar, Constraints on the deep structure and dynamic processes beneath the Alps and adjacent regions from an analysis of gravity anomalies, *Geophys. J. Int.*, 99, 19-32, 1989.

Matter, A., Sedimentologische Untersuchungen im östlichen Napfgebiet (Entlebuch - Tal der Grossen Fontanne, Kt. Luzern), *Eclogae Geol. Helv.*, 57, 315-428, 1964.

Matter, A., P. Homewood, C. Caron, D. Rigassi, J. Van Stujivenberg, M. Weidmann, and W. Winkler, Flysch and molasse of western and central Switzerland, in *Geology of Switzerland, a guidebook, Part B, Excursions*, edited by R. Trümpy, pp. 261-293, Schweiz. Geol. Komm., Basel, 1980.

Menkveld, J.W., Der geologische Bau des Helvetikums der Innerschweiz, 1, Text, Ph.D. thesis, 165 pp., Univ. of Bern, Bern, 1995.

Michalski, I., and M. Soom, The Alpine thermo-tectonic evolution of the Aar and Gotthard massifs, central Switzerland: Fission track ages on zircon and apatite and K-Ar mica ages, *Schweiz. Mineral. Petrogr. Mitt.*, 70, 373-387, 1990.

Milnes, A.G., and O.A. Pfiffner, Structural development of the Infrahelvetic Complex, eastern Switzerland, *Eclogae Geol. Helv.*,70, 83-95, 1977.

Milnes, A.G., and O.A. Pfiffner, Tectonic evolution of the Central Alps in the cross section St. Gallen-Como, *Eclogae Geol. Helv.*, 73, 619-633, 1980.

Müller, H.P., Geologische Untersuchungen in der subalpinen Molasse zwischen Einsiedeln und oberem Zürichsee (Kt. Schwyz), *Vjschr. Natf. Ges. Zürich*, 16, 153 pp., 1971.

Naef, H., P. Diebold, and S. Schlanke, Sedimentation und Tektonik im Tertiär der Nordschweiz, *NAGRA Tech. Ber.*, 85-14, 145 pp., Natl. Genoss. für die Lager. Radioaktiv. Abfälle, Baden, Switzerland, 1985.

Okaya, N., S. Cloetingh, and S. Müller, A lithospheric cross-section through the Swiss Alps, II, Constraints on the mechanical structure of a continent-continent collision zone, *Geophys. J. Int.*, 127, 399-414, 1996a.

Okaya, N., R. Freeman, E. Kissling, and S. Müller, A lithospheric cross-section through the Swiss Alps, I, Thermokinematic modelling of the Neoalpine orogeny, *Geophys. J. Int.*, 125, 504-518, 1996b.

Ottiger, R., M. Freimoser, H. Jäckli, J. Kopp, and E. Müller, *Geologischer Atlas der Schweiz , Blatt 131 pp., Zug (89)*, scale 1:25000, Schweiz. Geol. Komm., Basel, 1990.

Paola, C., P.L. Heller, and C.L. Angevine, The large-scale dynamics of grain-size variation in alluvial basins, 1, Theory, *Basin Res.*, 4, 73-90, 1992.

Peper, T., *Tectonic Control on the Sedimentary Record in Foreland Basins: Inferences From Quantitative Subsidence Analyses and Stratigraphic Modeling, CIP-Data*, 177pp., Koninklijke Bibl., Den Haag, Netherlands, 1993.

Pfiffner, O.A., Evolution of the north Alpine foreland basin in the Central Alps, in *Foreland Basins*, edited by P.A. Allen and P. Homewood, *Spec. Publ. Int. Assoc. Sedimentol.*, 8, 219-228, 1986.

Pfiffner, O.A., Alpine orogeny, in *The European Geotraverse*, edited by D. Blundell et al., pp. 180-189, Cambridge Univ. Press, New York, 1992.

Pfiffner, O.A., S. Sahli, and M. Stäuble, Structure and evolution of the external basement uplifts (Aar, Aiguilles Rouges/Mt. Blanc), in *Deep Structure of the Swiss Alps: Results of the National Research Program 20 (NRP 20)*, edited by O.A. Pfiffner et al., pp. 139-153, Birkhäuser, Boston, Mass., 1996.

Rahn, M., J. Mullis, K. Erdelbrock, and M. Frey, Very low-grade metamorphism of the Taveyanne greywacke, Glarus Alps, Switzerland, *J. Metamorph. Geol.*, 12, 625-641, 1994.

Rahn, M., J. Mullis, K. Erdelbrock, and M. Frey, Alpine metamorphism in the North Helvetic Flysch of the Glarus Alps, Switzerland, *Eclogae Geol. Helv.*, 88, 625-178, 1995.

Rey, D., T. Quarta, P. Mouge, M. Miletto, R. Lanza, A. Galdeano, M.T. Carozzo, E. Armando, and R. Bayer, Gravity and aeromagnetic maps on the western Alps: Contribution to the knowledge on the deep structures along the Ecors-Crop seismic profile, in *Deep Structure of the Alps*, edited by F. Roure et al., *Mém. Soc. Géol. France*, 156, 107-122, 1990.

Royden, L.H., The tectonic expression slab pull at continental convergent boundaries, *Tectonics*, 12, 303-325, 1993.

Schegg, R., The coalification profile of the well Weggis (Subalpine Molasse, central Switzerland): Implications for erosion estimates and the paleogeothermal regime in the external part of the Alps, *Bull. Ver. Schweiz. Pet. Geol. Ing.*, 61, 57-67, 1994.

Schlanke, S., Geologie der subalpinen Molasse zwischen Biberbrugg/SZ, Hütten/ZH und Aegerisee/ZG, Schweiz, *Eclogae Geol. Helv.*, 67, 243-331, 1974.

Schlunegger, F., A. Matter, and M.A. Mange, Alluvial fan sedimentation and structure of the southern Molasse Basin margin, Lake Thun area, Switzerland, *Eclogae Geol. Helv.*, 86, 717-750, 1993.

Schlunegger, F., D.W. Burbank, A. Matter, B. Engesser, and C. Mödden, Magnetostratigraphic calibration of the Oligocene to Middle Miocene (30-15 Ma) mammal biozones and depositional sequences of the Swiss Molasse basin, *Eclogae Geol. Helv.*, 89, 753-788, 1996.

Schlunegger, F., A. Matter, D.W. Burbank, and E.M. Klaper, Magnetostratigraphic constraints on relationships between evolution of the central Swiss Molasse Basin and Alpine orogenic events, *Geol. Soc. Am. Bull.*, 109, 225-241, 1997a.

Schlunegger, F., A. Matter, D.W. Burbank, W. Leu, M.A. Mange, and J. Màtyàs, Sedimentary sequences, seismofacies and evolution of the depositional systems of the Oligo/Miocene Lower Freshwater Molasse Group, Switzerland, *Basin Res.*, 9, 1-26, 1997b.

Schmid, S.M., and N. Froitzheim, Oblique slip and block rotation along the Engadine Line, *Eclogae Geol. Helv.*, 86, 569-593, 1994.

Schmid, S.M., H.R. Aebli, F. Heller, and A. Zingg, The role of the Periadriatic Line in the tectonic evolution of the Alps, in *Alpine Tectonics*, edited by M. Coward et al., *Geol. Soc. Spec. Publ. London*, 45, 153-171, 1989.

Schmid, S.M., O.A. Pfiffner, N. Froitzheim, G. Schönborn, and E. Kissling, Geophysical-geological transect and tectonic evolution of the Swiss-Italian Alps, *Tectonics*, 15, 1036-1064, 1996.

Schönborn, G., Alpine tectonics and kinematic models of the central Southern Alps, *Mem. Sci. Geol. Padova*, 44, 229-393, 1992.

Sinclair, H.D., Plan-view curvature of foreland basins and its implications for the palaeostrength of the lithosphere underlying the western Alps, *Basin Res.*, 8, 173-182, 1996.

Sinclair, H.P., and P.A. Allen, Vertical versus horizontal motions in the Alpine orogenic wedge: Stratigraphic response in the foreland basin, *Basin Res.*, 4, 215-232, 1992.

Sinclair, H.D., B.J. Coakley, P.A. Allen, and A.B. Watts, Simulation of foreland basin stratigraphy using a diffusion model of mountain belt uplift and erosion: An example from the central Alps, Switzerland, *Tectonics*, 10, 599-620, 1991.

Soom, M., Spaltspurdatierungen entlang des NFP 20-Westprofils (Externmassive und Penninikum), *Schweiz. Mineral. Petrogr. Mitt.*, 69, 191-192, 1990.

Speck, J., Geröllstudien in der subalpinen Molasse am Zugersee und Versuch einer paläogeographischen Auswertung, Ph.D. thesis, 175 pp., Univ. of Zürich, Zürich, Switzerland, 1953.

Stäuble, M., and O.A. Pfiffner, Processing interpretation and modeling of seismic reflection data in the Molasse Basin of eastern Switzerland, *Eclogae Geol. Helv.*, 94, 151-175, 1991.

Steck, A., and J. Hunziker, The Tertiary structural and thermal evolution of the Central Alps - Compressional and extensional structures in an orogenic belt, *Tectonophysics*, 238, 229-254, 1994.

Steiger, R., Dating of orogenic phases in the Central Alps by K-Ar ages of hornblende, *J. Geophys. Res.*, 69, 5407-5421, 1964.

Stürm, B., Die Rigischüttung. Sedimentpetrographie, Sedimentologie, Paläogeographie, Tektonik, Ph.D. thesis, 98 pp., Univ. of Zürich, Zürich, 1973.

Tanner, H., Beitrag zur Geologie der Molasse zwischen Ricken und Hörnli, *Mitt. Geol. Inst. Eidg. Tech. Hochsch. Zürich, C/22*, 108 pp., 1944.

Turcotte, D.L., and G. Schubert, Geodynamics: Application of continuum physics to geological problems, 650 pp., John Wiley, New York, 1982.

Vollmayr, T., and A. Wendt, Die Erdgasbohrung Entlebuch-1, ein Tiefenaufschluss am Alpennordrand, *Bull.*

Ver. Schweiz. Pet. Geol. Ing., 53, 67-79, 1987.

Wang, H., M. Frey, and W.B. Stern, Diagenesis and incipient metamorphism of the Helvetic Alps, eastern Switzerland: Clay mineral data, *Schweiz. Mineral. Petrogr. Mitt., 75*, 187-199, 1995.

Waschbusch, P.J., and L.H. Royden, Spatial and temporal evolution of foredeep basins: Lateral strength variations and inelastic yielding in continental lithosphere, *Basin Res., 4*, 179-196, 1992.

Watts, A.B., and W.B.F. Ryan, Flexure of the lithosphere and continental margin basins, *Tectonophysics, 36*, 25-44, 1976.

T.E. Jord:.n, Department of Earth Sciences, Cornell University, Snee Hall, Ithaca, NY 14853-1504. (e-mail: jor-dan@geology.cornell.edu)

E.M. Klaper, Geologisches Insitut, Universiät Bern, Baltzerstrasse 1, CH-3012 Bern, Switzerland. (e-mail: klaper@geo.unibe.ch)

Fritz Schlunegger, Insitut für Geowissenschaften, Friedrich-Schiller-Universität Jena, Burgweg 11, D-07749 Jena, Germany. (e-mail: fritz@geo.uni-jena.de)